

## Supplementary Information

# Laponite nanodisks "decorated" Fe<sub>3</sub>O<sub>4</sub> nanoparticles. A biocompatible nano-hybrid with ultrafast magnetic hyperthermia and MRI contrast agent ability

Georgia Basina,<sup>\*a,b</sup> George Diamantopoulos,<sup>b</sup> Eamonn Devlin,<sup>b</sup> Vassilis Psycharis,<sup>b</sup> Saeed M. Alhassan,<sup>c</sup> Michael Pissas,<sup>b</sup> George Hadjipanayis,<sup>a</sup> Aphrodite Tomou,<sup>b,d</sup> Alexandros Bouras,<sup>e</sup> Constantinos Hadjipanayis<sup>\*e</sup> and Vasileios Tzitzios<sup>\*b,c</sup>

<sup>a</sup>Department of Physics and Astronomy, University of Delaware, Newark, DE 19711, US.

<sup>b</sup>Institute of Nanoscience and Nanotechnology, NCSR Demokritos, 15310, Athens, Greece.

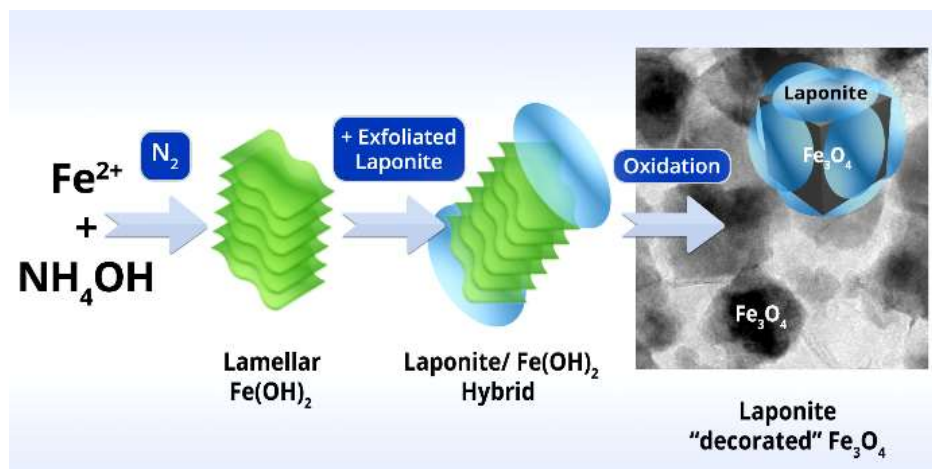
<sup>c</sup>Department of Chemical Engineering, Khalifa University, P.O. Box 127788, Abu Dhabi, United Arab Emirates.

<sup>d</sup>Goodfellow Cambridge Ltd., Ermine Business Park, Huntingdon PE29 6WR, Cambridge, UK.

<sup>e</sup>Brain Tumor Nanotechnology Laboratory, Department of Neurosurgery, Icahn School of Medicine at Mount Sinai, New York, NY.

### \* E-mails for correspondence:

v.tzitzios@inn.demokritos.gr; g.basina@inn.demokritos.gr; Constantinos.Hadjipanayis@mountsinai.org



## CONTENT:

Supplementary Information contains structural, magnetic and morphological characterization data based on XRD, VSM, TEM analysis of various Laponites “decorated” Fe<sub>3</sub>O<sub>4</sub> nanoparticles hybrids with 25 to 95 wt.% magnetic content. Summarized hydrodynamic diameter and Z-potential distribution histograms are also provided for the physicochemical characterization analysis of the prepared Fe<sub>3</sub>O<sub>4</sub>/Laponites nanohybrids. AFM images of the selected 50 wt.% Fe<sub>3</sub>O<sub>4</sub>/Laponite are presented. Finally, the temperature profile as a function of the field exposure time from various concentrations (5.5-22 mg/mL) colloidal solutions of 25, 50 and 75 wt.% Fe<sub>3</sub>O<sub>4</sub>/Laponite hybrids and literature review on SAR values as a function of the applied field frequency and strength of Fe-oxides based nanomaterials with various sizes and morphologies, are given for comparison.

1. **Fig. S1.** Powder XRD patterns of Laponite “decorated” Fe<sub>3</sub>O<sub>4</sub> nanoparticles hybrids with different magnetic loadings varied from 25 to 95 wt.% Fe<sub>3</sub>O<sub>4</sub>.
2. **Fig. S2.** Room temperature magnetic hysteresis loops of Laponite “decorated” Fe<sub>3</sub>O<sub>4</sub> nanoparticles hybrids with different magnetic loadings varied from 25 to 95 wt.% Fe<sub>3</sub>O<sub>4</sub>.
3. **Fig. S3.** Hydrodynamic diameter distribution histograms of Laponite “decorated” Fe<sub>3</sub>O<sub>4</sub> nanoparticles hybrids with different magnetic loadings varied from 25 to 95 wt.% Fe<sub>3</sub>O<sub>4</sub>.
4. **Fig. S4.** Z-potential distribution histograms of Laponite “decorated” Fe<sub>3</sub>O<sub>4</sub> nanoparticles hybrids with different magnetic loadings varied from 25 to 95 wt.% Fe<sub>3</sub>O<sub>4</sub>.
5. **Fig. S5.** TEM images of Laponite “decorated” Fe<sub>3</sub>O<sub>4</sub> nanoparticles with 25, 75, 90 and 95 wt.% Fe<sub>3</sub>O<sub>4</sub> content.
6. **Fig. S6.** AFM images of 50 wt.% Fe<sub>3</sub>O<sub>4</sub>/Laponite hybrid.
7. **Fig. S7.** Temperature profile as a function of field exposure time of various concentrations (5.5-22 mg/mL) for colloidal solutions of 25, 50 and 75 wt.% Fe<sub>3</sub>O<sub>4</sub>/Laponite hybrids.
8. **Table S1.** Summary literature data on specific absorption rate (SAR) values in Watts per Fe g as a function of the applied magnetic field frequency and strength for various Fe-oxides based nanomaterials with different size and morphology.

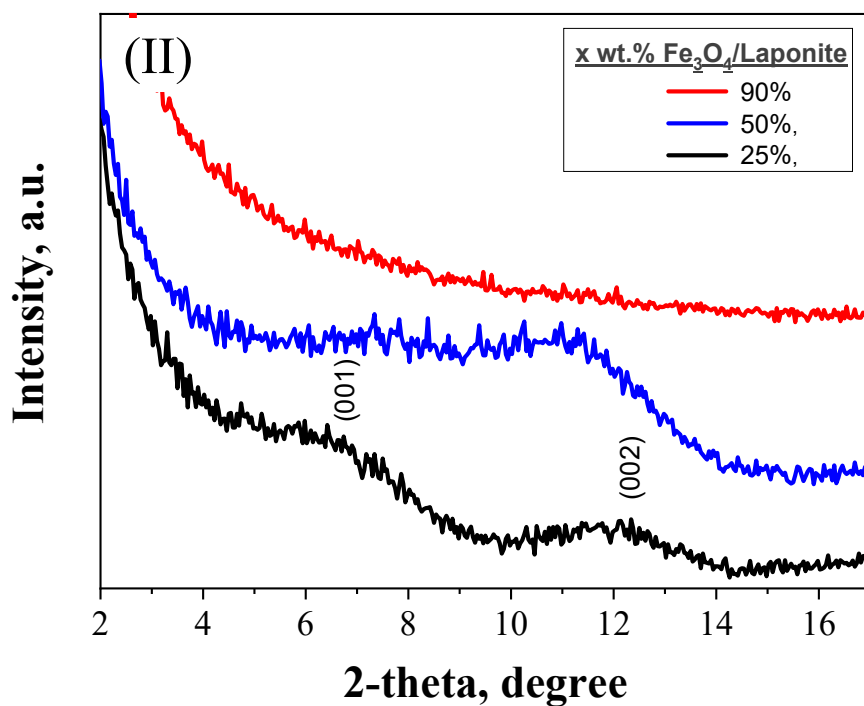
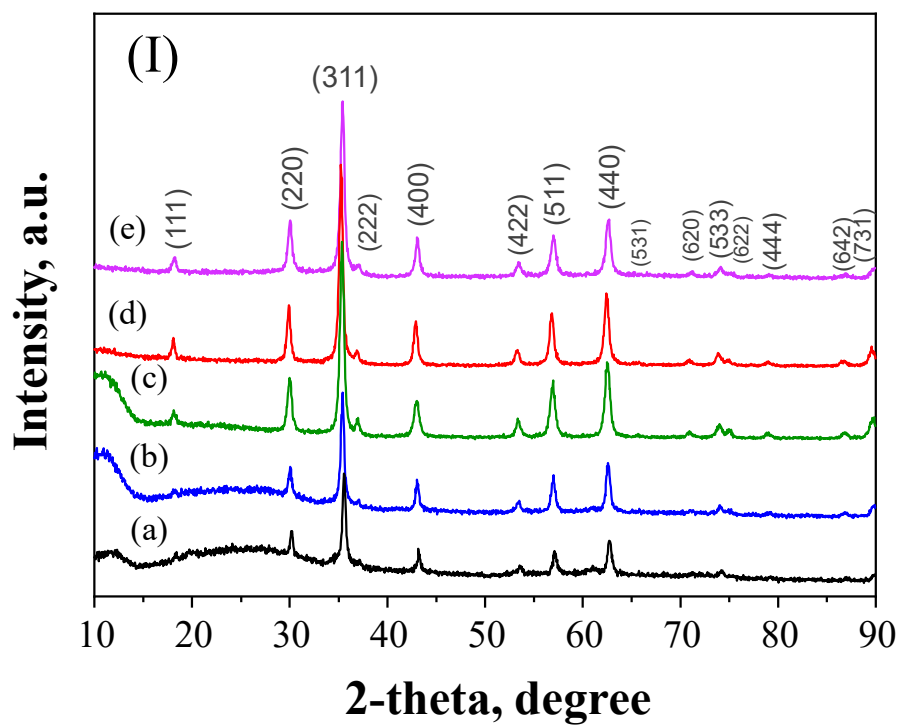


**Fig. S1.** Powder XRD patterns of the Laponite “decorated”  $\text{Fe}_3\text{O}_4$  nanoparticles hybrids with (a) 25, (b) 50, (c) 75, (d) 90 and (e) 95 wt.%  $\text{Fe}_3\text{O}_4/\text{Laponite}$ .

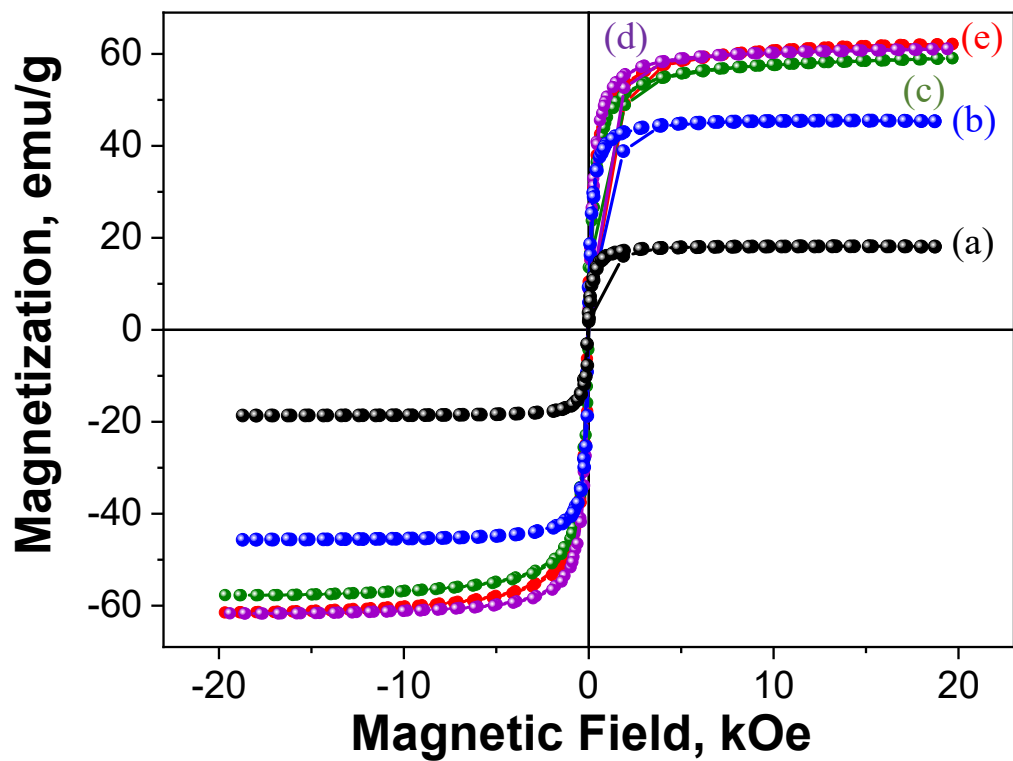


**Fig. S2.** Magnetic hysteresis loops at room temperature of the Laponite “decorated” Fe<sub>3</sub>O<sub>4</sub> nanoparticles hybrids with (a) 25, (b) 50, (c) 75, (d) 90 and (e) 95 wt.% Fe<sub>3</sub>O<sub>4</sub> content.

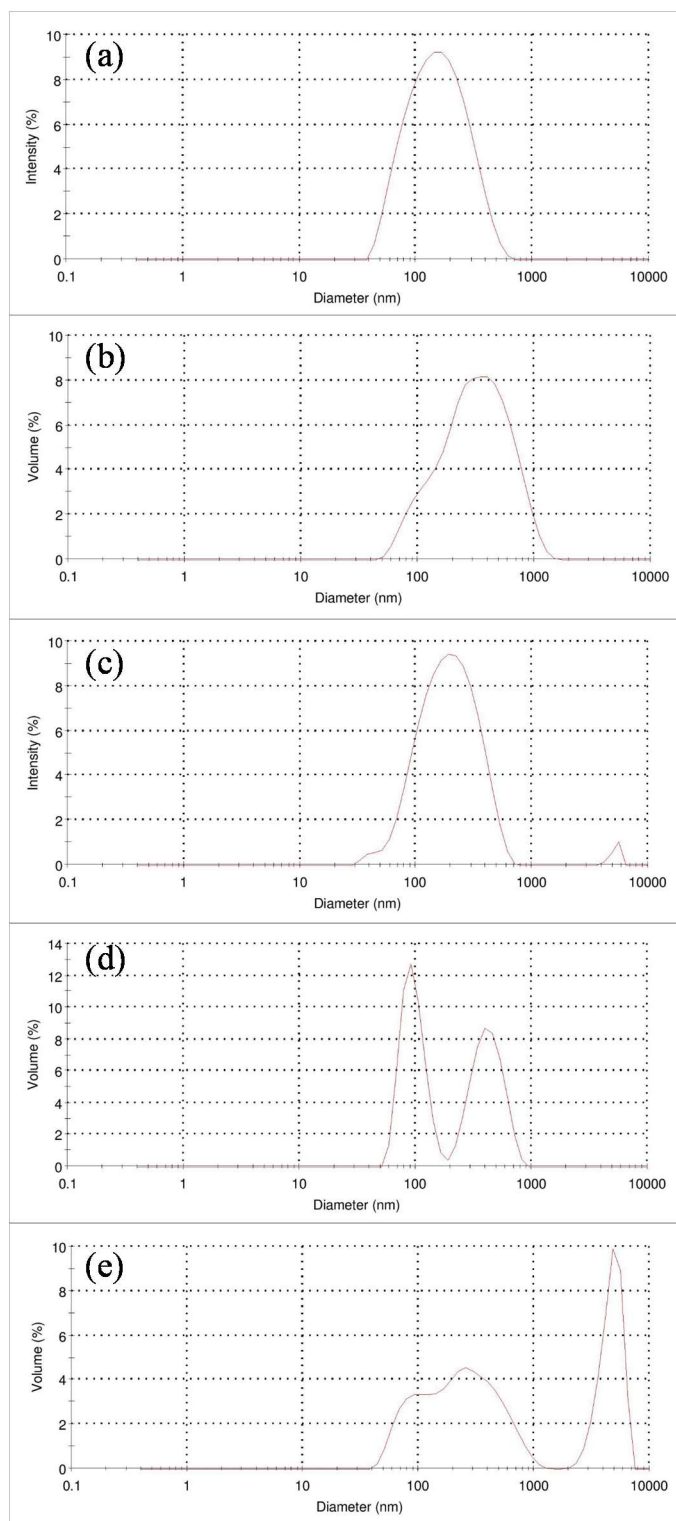


**Fig. S3.** Hydrodynamic diameter distribution histograms of Laponite “decorated” Fe<sub>3</sub>O<sub>4</sub> hybrids with 25, 50,75, 90, 95 wt.% Fe<sub>3</sub>O<sub>4</sub> nominal composition and respectively (a) 136, (b) 202.6, (c) 174, (d) 427.2 and 96.7 bimodal and (e) multimodal distribution.

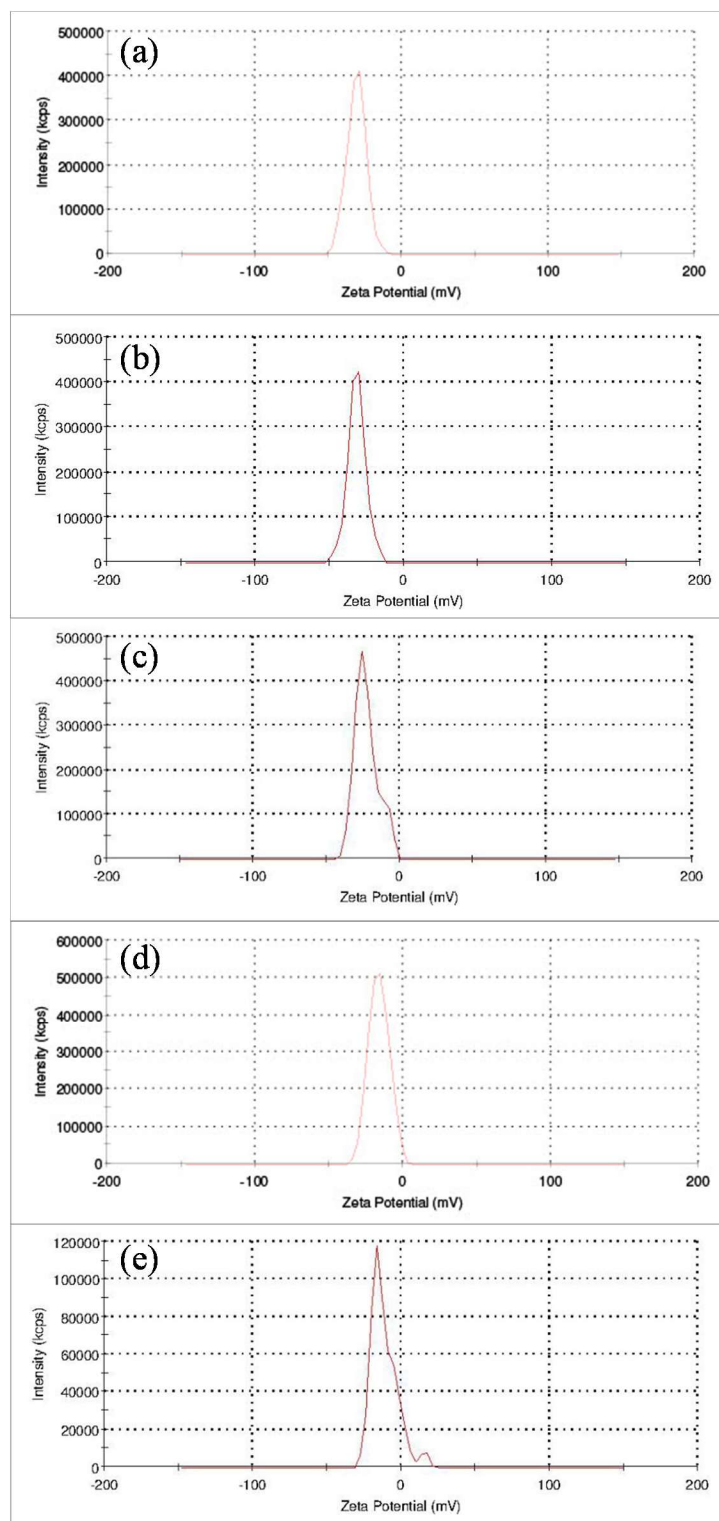


**Fig. S4.** Z-potential distribution histograms of Laponite decorated  $\text{Fe}_3\text{O}_4$  hybrids with 25, 50, 75, 90, 95 wt.%  $\text{Fe}_3\text{O}_4$  nominal composition and respectively values (a) -34.1 (b) -31.6 (c) -22.3, (d) -17.6, and (e) -11.4 mV.

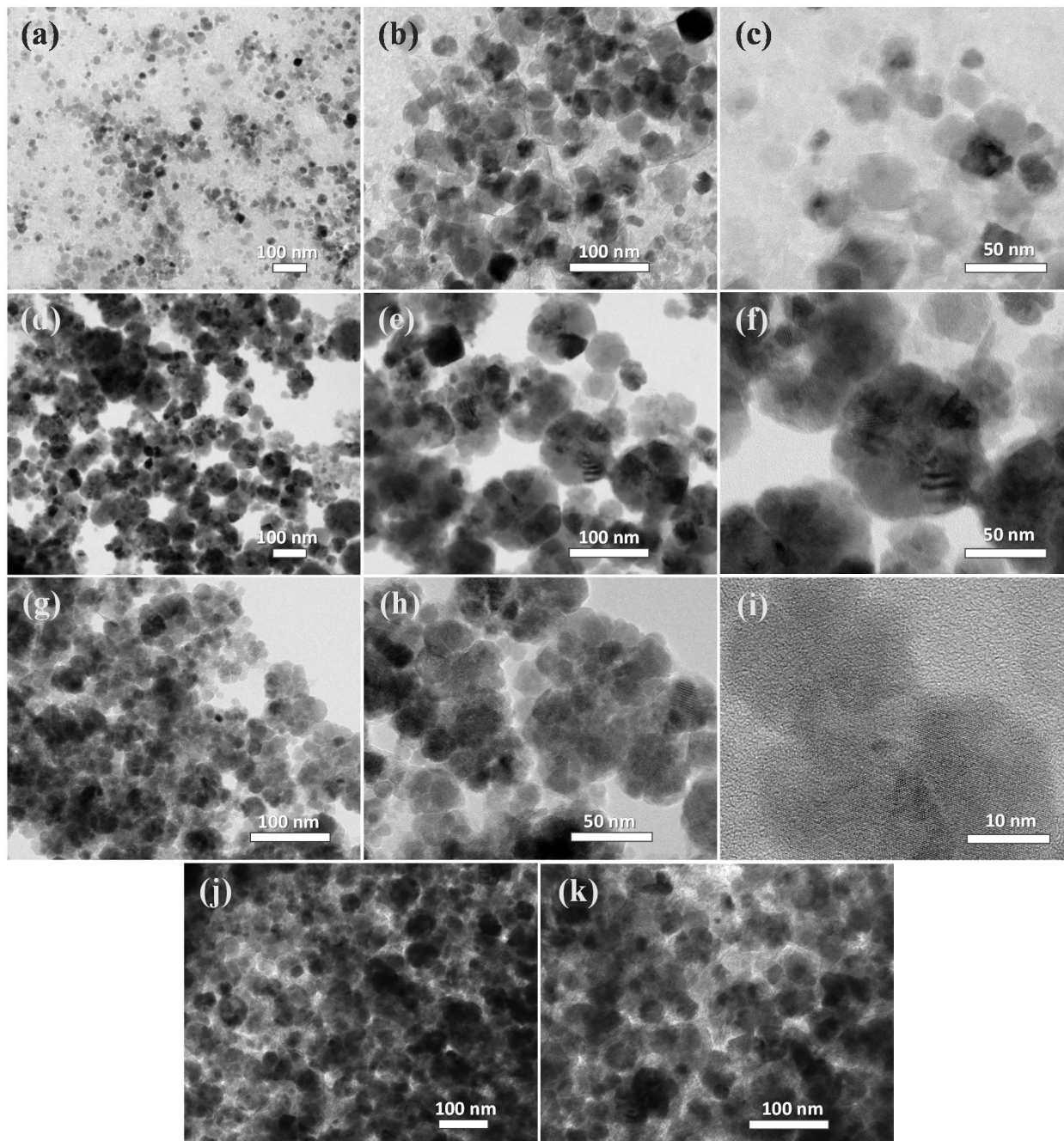


**Fig. S5.** TEM images of Laponite “decorated” Fe<sub>3</sub>O<sub>4</sub> nanoparticles with 25 wt.% (a-c), 75 wt.% (d-f), 90 wt.% (g-i) and 95 wt.% (j, k) Fe<sub>3</sub>O<sub>4</sub> content.

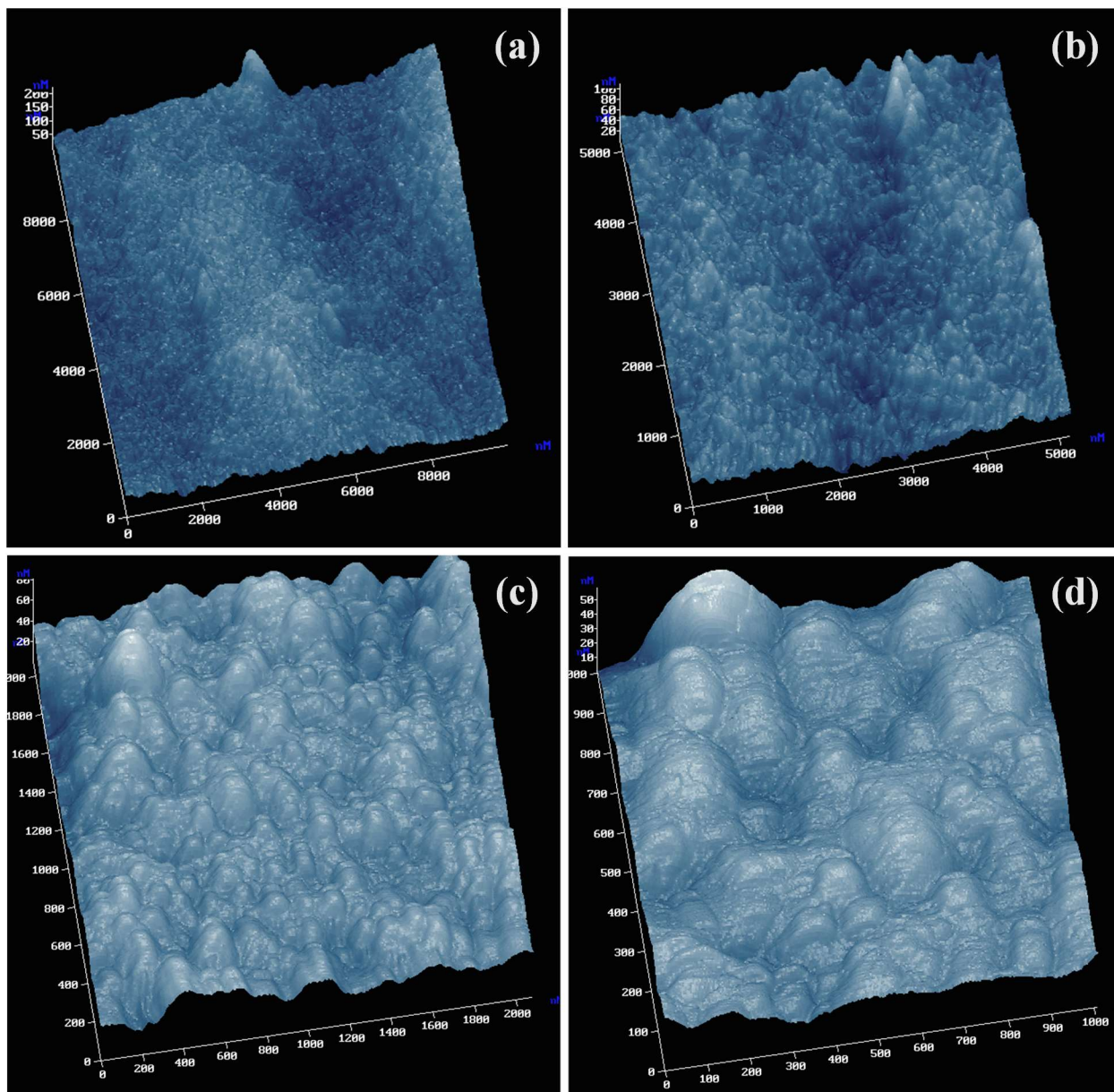


**Fig. S6.** AFM images of 50 wt.% laponite “decorated”  $\text{Fe}_3\text{O}_4$  hybrids.



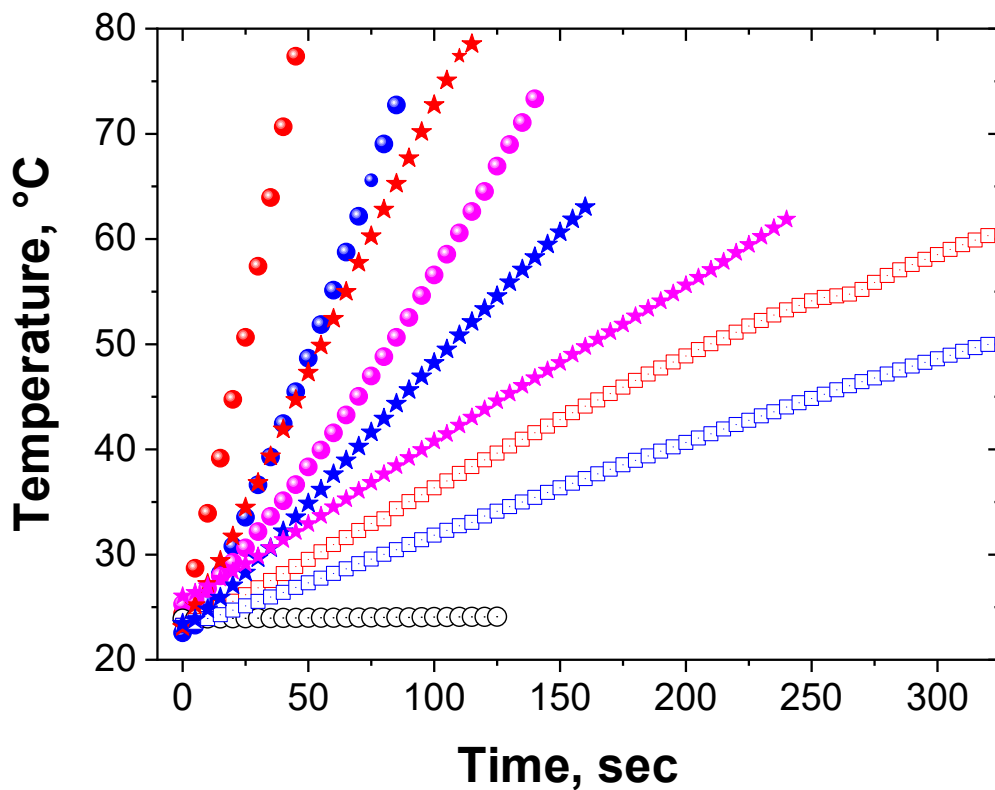


**Fig. S7.** Temperature profile as a function of field exposure time at 150 kHz and 28 kA/m for various  $\text{Fe}_3\text{O}_4$ /Laponites hybrids colloids of 25 wt.% (*squares*), 50 wt.% (*circles*) and 75 wt.% (*stars*)  $\text{Fe}_3\text{O}_4$  content with 22 mg/mL (*red*), 11 mg/mL (*blue*) and 5.5 mg/mL (*magenta*)  $\text{Fe}_3\text{O}_4$  concentration. Open circles DI water.

**Table S1. Summary literature data on specific absorption Rate (SAR) values in Watts per Fe g as a function of the applied magnetic field frequency and strength for various Fe-oxides based nanomaterials with different size and morphology.**

Material	Morphology	Stability	Particle diameter (nm)	Applied field (kA/m)	Frequency (kHz)	SAR, (W/g <sub>Fe</sub> )	Reference
<b>Fe<sub>3</sub>O<sub>4</sub></b>	cuboidal	excellent	20-40	28	<b>150</b>	540	<b>This work</b>
<b>Fe<sub>3</sub>O<sub>4</sub></b>	Cubes dimers and trimers		20	23.8	302	246	1
<b>Fe<sub>3</sub>O<sub>4</sub></b>	spherical	non coated low stability	6.8	40.1	265	203	2
<b>Co<sub>x</sub>Fe<sub>3-x</sub>O<sub>4</sub></b>	cubes	Toxicity issue Cobalt	20	32	105	915	3
<b>Iron oxide</b>	Cubes		19	29	700	2277	4
<b>Fe<sub>3</sub>O<sub>4</sub></b>	Assemblies		6	10	425	92.62	5
<b>Fe<sub>3</sub>O<sub>4</sub></b>	spherical		8	10	425	49.24	6
<b>Fe<sub>3</sub>O<sub>4</sub>/ Fe<sub>2</sub>O<sub>3</sub></b>	Faceted		18	11.94	300	86.87	7
<b>γ-Fe<sub>2</sub>O<sub>3</sub></b>	Multi-core		24	29	520	1500	8
<b>Fe<sub>3</sub>O<sub>4</sub></b>	aggregates		8.2	8	230	670	9
<b>γ-Fe<sub>2</sub>O<sub>3</sub></b>	spherical		16.5	24.7	700	1650	10
<b>γ-Fe<sub>2</sub>O<sub>3</sub></b>	Assemblies		50	25	765	400	11
<b>Fe<sub>3</sub>O<sub>4</sub></b>	cubes		35	21	168	76	12
<b>Fe<sub>3</sub>O<sub>4</sub></b>	rods		350	24.5	360	1045	13
<b>Fe<sub>3</sub>O<sub>4</sub></b>	irregular		8-10	35.8	316	130	14
<b>Fe<sub>3</sub>O<sub>4</sub>/ Fe<sub>2</sub>O<sub>3</sub></b>	tubes		300	36.1	107	465	15
<b>Fe<sub>3</sub>O<sub>4</sub>/Fe<sub>2</sub>O<sub>3</sub></b>	rings		207	36.1	107	340	
<b>Fe<sub>3</sub>O<sub>4</sub>/Fe<sub>2</sub>O<sub>3</sub></b>	branched		29	24.5	488	457	16

## REFERENCES:

1. D. Niculaes, A. Lak, G. C. Anyfantis, S. Marras, O. Laslett, S. K. Avugadda, M. Cassani, D. Serantes, O. Hovorka, R. Chantrell and T. Pellegrino, *ACS Nano*, 2017, **11**, 12121-12133.
2. M. E. de Sousa, M. B. Fernández van Raap, P. C. Rivas, P. Mendoza Zélis, P. Girardin, G. A. Pasquevich, J. L. Alessandrini, D. Muraca and F. H. Sánchez, *The Journal of Physical Chemistry C*, 2013, **117**, 5436-5445.
3. A. Sathya, P. Guardia, R. Brescia, N. Silvestri, G. Pugliese, S. Nitti, L. Manna and T. Pellegrino, *Chemistry of Materials*, 2016, **28**, 1769-1780.
4. P. Guardia, R. Di Corato, L. Lartigue, C. Wilhelm, A. Espinosa, M. Garcia-Hernandez, F. Gazeau, L. Manna and T. Pellegrino, *ACS Nano*, 2012, **6**, 3080-3091.
5. K. C. Barick, M. Aslam, Y.-P. Lin, D. Bahadur, P. V. Prasad and V. P. Dravid, *Journal of Materials Chemistry*, 2009, **19**, 7023-7029.
6. S. Nigam, K. C. Barick and D. Bahadur, *Journal of Magnetism and Magnetic Materials*, 2011, **323**, 237-243.
7. Y. V. Kolen'ko, M. Bañobre-López, C. Rodríguez-Abreu, E. Carbó-Argibay, A. Sailsman, Y. Piñeiro-Redondo, M. F. Cerqueira, D. Y. Petrovykh, K. Kovnir, O. I. Lebedev and J. Rivas, *The Journal of Physical Chemistry C*, 2014, **118**, 8691-8701.
8. L. Lartigue, P. Hugounenq, D. Alloyeau, S. P. Clarke, M. Lévy, J.-C. Bacri, R. Bazzi, D. F. Brougham, C. Wilhelm and F. Gazeau, *ACS Nano*, 2012, **6**, 10935-10949.
9. K. Hayashi, M. Moriya, W. Sakamoto and T. Yogo, *Chemistry of Materials*, 2009, **21**, 1318-1325.
10. J.-P. Fortin, C. Wilhelm, J. Servais, C. Ménager, J.-C. Bacri and F. Gazeau, *Journal of the American Chemical Society*, 2007, **129**, 2628-2635.
11. D. Sakellari, K. Brintakis, A. Kostopoulou, E. Myrovali, K. Simeonidis, A. Lappas and M. Angelakeris, *Materials Science and Engineering: C*, 2016, **58**, 187-193.
12. L. Lartigue, C. Innocenti, T. Kalaivani, A. Awwad, M. d. M. Sanchez Duque, Y. Guari, J. Larionova, C. Guérin, J.-L. G. Montero, V. Barragan-Montero, P. Arosio, A. Lascialfari, D. Gatteschi and C. Sangregorio, *Journal of the American Chemical Society*, 2011, **133**, 10459-10472.
13. Y. Yang, M. Huang, J. Qian, D. Gao and X. Liang, *Scientific Reports*, 2020, **10**, 8331.
14. A. Rajan, M. Sharma and N. K. Sahu, *Scientific Reports*, 2020, **10**, 15045.
15. G. Niraula, J. A. H. Coaquira, G. Zoppellaro, B. M. G. Villar, F. Garcia, A. F. Bakuzis, J. P. F. Longo, M. C. Rodrigues, D. Muraca, A. I. Ayesh, F. S. M. Sinfrônio, A. S. de Menezes, G. F. Goya and S. K. Sharma, *ACS Applied Nano Materials*, 2021, **4**, 3148-3158.
16. N. H. AbuTalib, A. P. LaGrow, M. O. Besenhard, O. Bondarchuk, A. Sergides, S. Famiani, L. P. Ferreira, M. M. Cruz, A. Gavriilidis and N. T. K. Thanh, *CrystEngComm*, 2021, **23**, 550-561.